Indian Journal of Chemistry
Vol. 63, June 2024, pp. 621-627
DOI: 10.56042/ijc.v63i6.9807

Investigation of the antimicrobial applications of nanosized zinc ferrite synthesised by green route

Arunkumar Lagashetty*[a], Chaitranjali[a], Sangeetha J[a], Kavya G[a], Nandish K[a], Nasareen H[a], Pooja A[a], Veena V[b], Preeti R K[c] & Sangappa K Ganiger[d]

[a] Department of Chemistry, Vijayanagara Sri Krishnadevaraya University, Ballari 583 105, Karnataka, India
[b] Department of Chemistry, Ballari Institute of Technology & Management, Ballari 583 105, Karnataka, India
[c] Department of Zoology, Gulbarga University, Kalaburagi 585 103, Karnataka, India
[d] Department of Physics, Government Engineering College, Huvinahadagali 583 219, Karnataka, India
E-mail: arun.lagashetty@gmail.com

Received 22 March 2024; accepted (revised) 22 May 2024

Green synthetic method for bimetallic oxide nanomaterials by biological reduction method using plant extract has become an attentive research approach due to its easy, efficient and eco-friendly system. An attempt has been made to synthesize nanosized zinc ferrite bi-metallic oxide ($ZnFe_2O_4$) nanomaterials using *Ficus benghalensis* plant leaf extract by bio-reduction method. The structural and morphological characterisation of prepared zinc ferrite sample is carried out by X-ray diffraction (XRD) and scanning electron microscope (SEM) tools, respectively. Bonding nature of the sample is studied by Fourier transfer infrared (FT-IR) tool. Presence of metal confirmation in the prepared sample is identified by EDX analysis. Antimicrobial activity of the sample is also carried out for its antibacterial and antifungal behaviour.

Keywords: $ZnFe_2O_4$, *Ficus benghalensis*, XRD, SEM, FT-IR, EDX

Magnetic oxide nanoparticles are attracted to recent researchers due to their extensive applications, ranging from fundamental research to industrial use[1,2]. Spinal ferrite nanocrystals are regarded as the most important inorganic nanomaterials because of their electronic, optical, electrical, magnetic, and catalytic properties[3-6]. The biological methods for material synthesis at the nano scale levels are in accordance with the eco-friendly system, thus avoiding huge consumption of fuel[7]. Green route is presenting a different way of thinking in chemistry intended to eliminate the entry of harmful products to the environment[8]. This method is a bottom-up approach also for chemical reduction by the use of extract as a natural product. In addition, it avoids the production of unwanted or harmful by-products through the build-up of reliable, sustainable, and eco-friendly system. Metal spinal ferrite nanoparticles have the general molecular formula MFe_2O_4 (*e.g.*, M=Zn, Ni, Co, Mn, or Mg), and they have a face-cantered-cubic (FCC) close packing structure. Among the spinel ferrite compounds, $ZnFe_2O_4$ has been studied extensively due to its high electromagnetic performance, excellent chemical stability, mechanical hardness, low coercivity, and moderate saturation magnetization, which make it a good conductor for applications as soft magnets and low-loss materials at high frequencies[9-12].

Zinc ferrite is an inorganic compound composed by zinc and iron oxides in which its properties are dependent on the chemical composition and microstructural characteristics of both oxides[13-15]. Literature review reveals various synthetic methods of zinc ferrite nanocrystals in which green route records for its simplicity[16,17]. Different methods have achieved the required sizes and shapes and also reduce harmful products to the environment [18,19]. The magnetic as well as other properties of zinc ferrite, especially in nano fraction, make that is applicable for a range of applications[20,21]. Zinc ferrite nanoparticles have shown potential to be used in biomedical field such as magnetic resonance imaging, drug delivery, *etc.*[22-24]. In order to achieve materials that have the desired physical and chemical properties, the preparation of zinc ferrite nanocrystals through different routes has become an essential focus of the related research and development activities[25].The requirement for environmentally friendly nontoxic synthesis protocols for nanoparticle synthesis has led to a developing interest in biological approaches that are free from

toxic chemicals formed as by products[26,27]. Thus, there is an increase in demand for green nanotechnology; multiple biological approaches for both extra cellular and intracellular nanoparticles synthesis have reported using microorganisms, including bacteria, fungi and plants[28-30]. The plant leaf extract or parts of this plant shows antimicrobial and other medicinal properties such as antioxidant, analgesic, and anti-inflammatory activities. Furthermore, the content of the plant leaf extract has a reduction property; hence, it is used for synthesis of metal oxide nanoparticles by reduction reactions[31,32]. Researchers have successfully experimented with different metal oxide nanoparticle prepared by biological routes[33]. However, very few bimetallic oxide particles have been reported using a green synthesis route[34].

In the present study, zinc ferrite nanocrystals were prepared from an aqueous solution containing metal salts, plant extract and deionized water using bio-reduction method. No other chemicals were added to the solution for its final oxide nanomaterials. This method is environmentally friendly procedure, it neither uses nor produces toxic substances, and it offers the advantages of simplicity, low cost, and low reaction temperatures. The textural and morphological characteristics of the zinc ferrite nanocrystals were studied with various techniques to determine the influence of calcination temperature on the crystallization, morphology, and particle size distribution of the nanocrystals to explore its parameters of interest. Antimicrobial activity studies were carried out by the reference of standard method for its biological behaviour.

Experimental Section

The required chemicals used in the present experimentation are of AR grade and are purchased from Merck (Mumbai, India). Properly rinsed glass wares with chromic acid are used in the experimentation. Green derivation of zinc ferrite was carried out by biological reduction method using *Ficus benghalenesis* plant leaf extract. Agar-well diffusion method is used for antibacterial activity study.

Preparation of leaf extract

Fresh *Ficus benghalenesis* plant leaf (Fig. 1(a)) were collected in early morning from VSK university campus and washed thoroughly with distilled water. 10gm of these leaves were weighed, crushed and mixed with 50 mL distilled water in 100 mL conical flask. The content was heated for 10 min and cooled to RT. Mixture was filtered through Whatmann filter paper to get plant leaf extract as shown in Fig. 1(b).

Fig. 1 — Optical image of *Ficus benghalenesis* plant a) leaf b) leaf extract

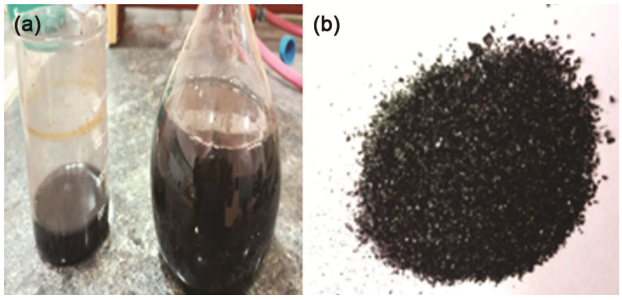

Fig. 2 — Optical image of (a) Reaction mixture (b) Zinc ferrite sample

Synthesis of zinc ferrite nanoparticle

Prepare 0.001M zinc sulphate ($ZnSO_4$) and ferrous sulphate ($FeSO_4$) solutions in double distilled water in separate container. 15 mL of these prepared solutions were mixed with each other in another container. Further, added the above prepared 15 mL of *Ficus bengalensis* aqueous leaf extract to the above salt solution mixture followed by heating the solution on hot plate at 60°C for about 15 min. Cool the solution to RT for about 24 h. Dark brownish colour is obtained due to complete reduction of metal salts (Figure-2(a)). During the synthesis process, the Zn^{2+} and Fe^{2+} ions reduces to its metals by use of organic content of the plant leaf extract. Then centrifuged the solution at 10,000 rpm for about 10 min and is re-dispersed in water so as to get the yield 0.1g of the sample[35] and is shown in Fig. 2(b). Possible reactions taking place in the synthetic scheme are given below.

$Zn^{2+}SO_4^{2-}.2H_2O$ + Plant extract $\rightarrow Zn^0$NPS + Byproducts

$Fe^{2+}SO_4^{2-}.2H_2O$ + Plant extract $\rightarrow Fe^0$NPS + Byproducts

$Zn^0NPS + Fe^0NPS + Plant\ extract \rightarrow ZnFe_2O_4NPS$

Biological Activity

Antibacterial activity

Antibacterial activity of different compounds was tested by agar well diffusion assay[36]. Petri dishes were prepared by pouring 20 mL of sterilized NA media under aseptic condition and allowed to solidify. After solidification of the media, 100 µL of standardized test microbial inoculums of Gram-positive bacteria *S. aureus*, *B. subtilis* and Gram-negative bacteria and *S. typhi*, *Pseudomonas aeruginosa* were spread uniformly using sterile cotton swabs. 6 mm diameter agar is drawn from plate to form a well using sterile cork borer. Antibiotic gentamycin was used as positive control, DMSO as negative control. After keeping at 4°C for 4 h for the diffusion of antibacterial metabolites, thereafter plates were incubated at 37°C for 24 h. The diameter of the inhibition zone around the well is measured in millimetre (mm) and the average of three repeated agar discs were taken to assess the strength of antibacterial activity[37].

Antifungal activity

Petri dishes were prepared by pouring 20 mL of sterilized PDA media under aseptic condition and allowed to solidify. After solidification of the media, 100 µL of standardized test *Aspergillus niger* and *Fusarium* was spread uniformly using sterile L-shaped loop. 6 mm diameter agar is drawn from plate to form a well using sterile cork borer. Antifungal Nystatin was used as positive control, DMSO as negative control. After keeping at 4°C for 4 h for the diffusion of antibacterial metabolites, thereafter plates were incubated at 28ºC for 72 h. The diameter of the inhibition zone around the well is measured in millimetre (mm) and the average of three repeated agar discs were taken to assess the strength of antifungal activity[38].

Characterization Techniques

The powder X-ray diffraction patterns were recorded on a JEOL JDX-8P diffractometer using CuKα radiation (1.54 Å) at 30 kV. The Fourier transform infrared (FT-IR) spectra of the samples were recorded on a Perkin-Elmer FT-IR (Model No. 1000) in the range 4000-400 cm^{-1} at a resolution of 4 cm^{-1}. JEOL JSM-6380 LA scanning electron microscope with energy dispersive micro analysis of X-Ray (EDAX) is used to study particle morphology with metal confirmation of the sample.

Results and Discussion

Visual observation of colour change

Physical confirmation of the synthesized zinc ferrite sample was done by visual observation of the colour change in the solution. Fig. 1(b) shows that, the *Ficus benghalenesis* plant leaf extract is in very light yellowish colour whereas salt solutions show colourless solutions. Mixture of these three solutions shows dark brownish colour solution (Fig. 2(a)) due to biological reduction of salt solution leading to the formation of zinc ferrite.

UV-Visible study

UV-visible study is the most widely used technique for the sample analysis by identifying the possible absorption. For the successful synthesis process, this stands a testimony for robust evidence. The reaction progress between Zn ion and Fe ions and leaf extract was monitored by UV spectral study in aqueous product solution. Fig. 3 shows the UV-vis spectrum of a synthesised zinc ferrite nanoparticle sample. This Fig. indicates the presence of single surface plasmon absorption band at 500 nm and is the only maximum absorption band in the spectrum that corresponds to $ZnFe_2O_4$ sample. It also proved the nature of bimetallic nanoparticles. The forming of colloidal gel solution that contains both Zn and Fe is indicated by the shifting towards red side. Reduction of metal ions and formation of stable ferrite nanoparticles occurred rapidly in short span of time[39].

FT-IR study

It is known fact that in normal ferrites both absorption bands depend on the nature of the sample. The synthesised sample was examined using FT-IR

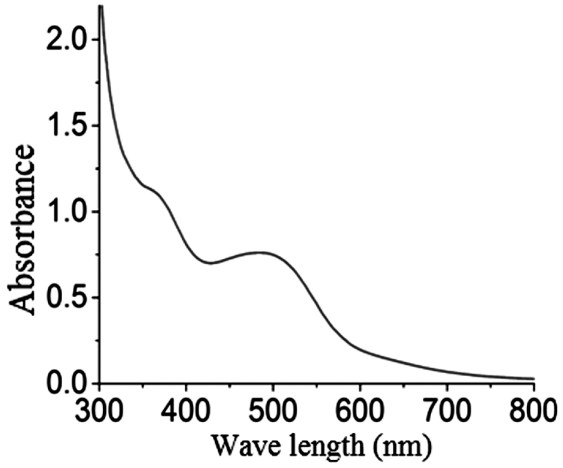

Fig. 3 — UV visible spectrum of $ZnFe_2O_4$ NPs

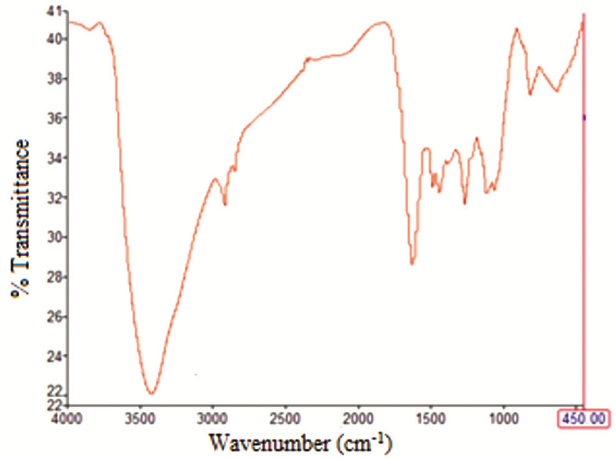

Fig. 4 — FT-IR spectrum of $ZnFe_2O_4$ NPs

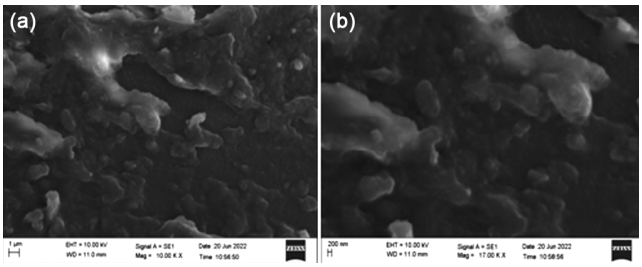

Fig. 5 — SEM image of $ZnFe_2O_4$ at (a) Low resolution (b) High resolution

spectroscopy to identify the vibrational bonding nature. Fig. 4 shows FT-IR spectrum of the green derived zinc ferrite nanoparticle sample. A broad band at 3300 cm^{-1} corresponds to the presence of octahedral OH^- group indicating moisture content in the sample. The vibrations correspond to the spinal structure as well absorbed at around 2926 cm^{-1} indicating the alkane -CH stretching and peak at 1623 cm^{-1} indicates -C-O stretching. The absorption peaks located below 1000 cm^{-1} corresponding to Fe-O and ZnO stretching vibrational frequency. This spectral data confirms the formation of zinc ferrite sample[40]. The main absorption band of zinc ferrite sample has a high intensity and a rapid shift to the wave number below 1000 cm^{-1}, which corresponds to the metal oxygen bands stretching vibrations (Zn-O-Fe). The appearance of these bonding groups proves that the synthesis of zinc ferrite by green route.

SEM study

Morphological conformation of synthesized $ZnFe_2O_4$ nanoparticles was carried out by scanning electron microscope tool. Fig. 5(a-b) shows SEM image of $ZnFe_2O_4$ sample at low and high resolution

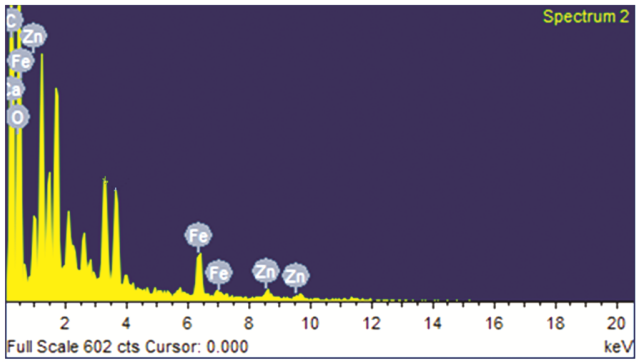

Fig. 6 — EDX Spectra of $ZnFe_2O_4$ NPs

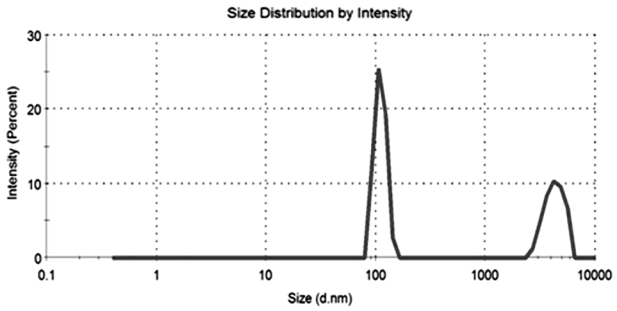

Fig. 7 — XRD pattern of$ZnFe_2O_4$ NPs

respectively. Images clearly indicates that microstructure of grains of the sample are ultra-small in size. Most of the grains containing a large number of atoms have very small dimensions. The fine spherical particles with different sized particles are observed in the image. In addition, most of the particles seem to be close assembles in a close compact structure with irregular particle size. Particles agglomeration with applicable orientation morphology is also observed in high resolution image.

EDX study

Compositional analysis of the samples was done by energy dispersive X-ray spectroscopic technique. The EDX technique supplies the effective atomic concentration of different constituents on top surface layers of the solid investigated. Fig. 6 shows EDX pattern of $ZnFe_2O_4$ NPs. The pattern shows that the presence of Fe, Zn and O elemental signals confirm the formation of $ZnFe_2O_4$ nanoparticles. This indicates that the expected stoichiometry under preparation is well maintained in the sample prepared using green method.

XRD study

Fig. 7 shows the indexed XRD pattern of green readied $ZnFe_2O_4$ NPs sample. It is observed from the

pattern that the XRD pattern shows (220) (311) (400) (422) and (511) sharp reflections, which are indexed in the pattern. Each of these peaks in the pattern is sharp and extreme. In addition, the pattern indicates the presence of sharp Bragg reflections representing the crystalline nature of sample. The main diffraction peaks are attributed to the plane showing the characteristics of a single phase cubic spinal structure. Observed diffraction peaks are fairly in good agreement with those of standard patterns for the face centred cubic structure of JCPDS card No. 22-2012 for $ZnFe_2O_4$. It is also observed that there are no additional peaks in the above pattern suggesting that the prepared sample do not have any secondary phase formation in the prepared sample[41]. So that, the pattern does not demonstrate any extra peak other than above referenced confirming the high immaculateness of the sample.

DLS study

Fig. 8 shows the DLS spectrum of $ZnFe_2O_4$ NPs. Dynamic light scattering characterization was used to determine the size and distribution of $ZnFe_2O_4$ NPs. The Fig. shows the size of the prepared $ZnFe_2O_4$ sample distributed on the DLS spectrum was 109 nm.

Biological activity of $ZnFe_2O_4$ NPs

Antibacterial assay

Fig. 9 shows antibacterial activity of the compound. It was tested by agar well diffusion assay with some modifications. Petri dishes were prepared by pouring 20 mL of sterilized NA media under aseptic condition and allowed to solidify. After solidification of the media, 10 µl of standardized test microbial inoculums of gram-positive bacteria *s. aureus*, *B. subtilis* and Gram- negative bacteria and *S. Typhi*, *pseudomonas aeruginosa* were spread uniformly using sterile cotton swabs. 6 mm diameter agar is drawn from plate to form a well using sterile cork borer. Antibiotic gentamycin was used as positive control, DMSO as negative control. After keeping at 4°C for 4 h for the diffusion of antibacterial metabolites, thereafter plates were incubated at 37°C for 24 h. The diameter of the inhibition zone around the well measured in mm and the average of three repeated agar discs were taken to assess the strength of antibacterial activity[42]. Antibacterial activity is shown in Reference Table 1.

The antibacterial activity of green synthesized $ZnFe_2O_4$ NPs was qualitatively measured by performing test against pathogenic microorganisms

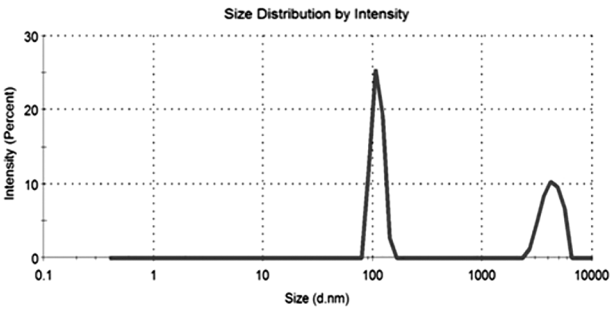

Fig. 8 — DLS spectrum of $ZnFe_2O_4$ NPs

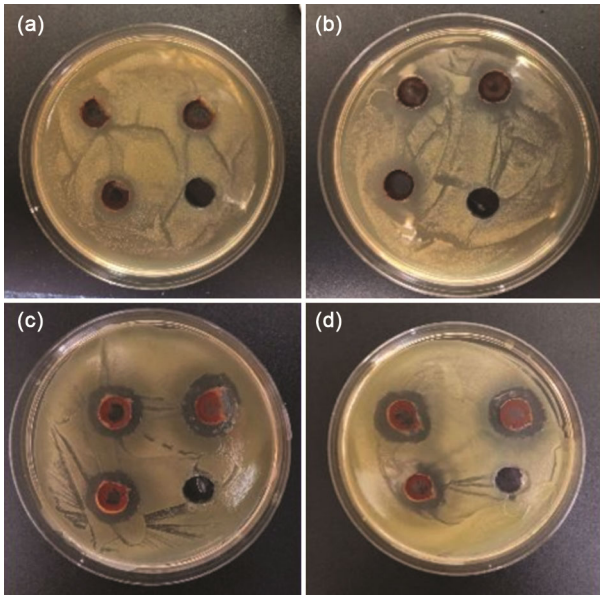

Fig. 9 — Antibacterial activities against pathogenic bacteria : a) *S. aureus b) B. subtilis* c) *S. Typhi*, d) *Pseudomonas aeruginosa*

Table 1 — Antibacterial activity reference table.

$ZnFe_2O_4$NPs Dose	*S. aureus*	*B. subtilis*	*S. Typhi*,	*P. aeruginosa*
10 µgmL^{-1}	8 ± 0.8	10 ± 0.5	8 ± 0.5	10 ± 0.8
50 µgmL^{-1}	10 ± 0.5	11 ± 0.5	10 ± 0.5	12± 0.5
100 µgmL^{-1}	12 ± 0.5	13 ± 0.5	11 ± 0.5	13 ± 0.5
Gentamycin	14 ± 0.5	16 ± 0.5	15 ± 0.5	16 ± 0.5

against *S. aureus*, *B. subtilis*, *S. Typhi and Pseudomonas aeruginosa*. The absence of growth around the nanoparticle is an indirect measure of the ability of the material to inhibit the bacteria growth. The zone inhibition produced by the nanoparticle against the gram negative and the gram positive bacteria is shown in Fig. 9. The effect of $ZnFe_2O_4$ NPs on bacterial linear growth revealed that the bacterial growth was decreased by increasing the concentrations of the nanoparticles. The antimicrobial activity of the nanoparticles is known to be the

function of surface area which is adhesion to the microorganisms. The small size and the high surface to volume ratio *i.e*., large surface area enhances the interaction between the nanoparticles and the microbes to carry out a broad range of probable antimicrobial activities. The bacterial wall of Gram-negative bacteria is composed of a specific arrangement of lipid A, lipopolysaccharides and peptidoglycans less than 15 nm thick. However, Gram-positive bacteria contain mainly very thick peptidoglycans with a cell wall of ~ 80 nm, which acts as a boundary layer, protecting the large molecules such as protein to be easily leaked out after disruption of the cell membrane[43-44].The green synthesised $ZnFe_2O_4$ NPs have larger surface area due to smaller size that bring the disruption of bacterial cell membrane which could lead to leakage of cytoplasmic materials (*e.g*., minerals, proteins, and genetic materials) and eventually causing bacterial death. Our present investigation demonstrates that $ZnFe_2O_4$ NPs treatment can cause membrane disruption in both gram-negative and gram-positive strains, and can lead to bacterial death through cell membrane damage.

Antifungal activity

Fig. 10 shows antifungal activity of different compounds. It was tested by agar well diffusion assay with some modifications. Petri dishes were prepared by pouring 20 mL of sterilized PDA media under aseptic condition and allowed to solidify. After solidification of the media, 100µl of standardized test *Aspergillus niger* and *Fusarium S* was spread uniformly using sterile L-shaped loop. 6 mm diameter agar is drawn from plate to form a well using sterile cork borer. Antifungal Nystatin was used as positive control, DMSO as negative control. After keeping at 4°C for 4 h for the diffusion of antibacterial metabolites, thereafter plats were incubated at 28°C for 72 h. The diameter of the inhibition zone around the well is measured in mm and the average of three repeated agar discs were taken to assess the strength of antibacterial activity[45]. The Table 2 shows antifungal activity reference

Antifungal activity of green $ZnFe_2O_4$ NPs was tested by following disc diffusion method. The presence of significant inhibition zones (ZoI) indicated the anti-fungal effect of $ZnFe_2O_4$ NPs. In the present study, effect of different concentrations of green $ZnFe_2O_4$ NPs (10 to 100 µg/mL) was evaluated against *Aspergillus niger* and *Fusarium S* fungus. Observed difference in the zone of inhibitions for

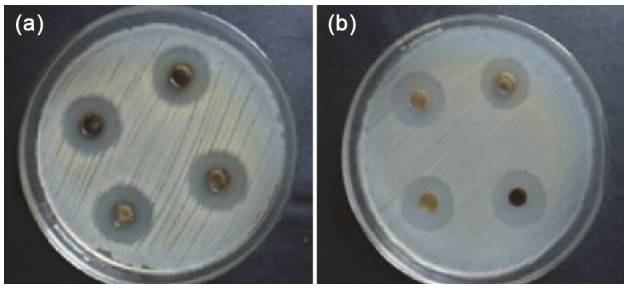

Fig. 10 — Antifungal activity of a) *Aspergillus niger* b) *Fusarium*

Table 2 — Antifungal activity reference table

Sl. No	*Anti-fungal* $ZnFe_2O_4$ NPs Dose	*Aspergillus niger*	*Fusarium S*
1	10 µgmL^{-1}	8 ± 0.8	9 ± 0.8
2	50 µgmL^{-1}	12 ± 0.2	13 ± 0.1
3	100 µgmL^{-1}	16 ± 0.1	16 ± 0.9
4	Nystatin	20 ± 0.4	21 ± 0.5

antifungal activity can be attributed to the structural differences between the fungal strains. The obtained result suggests that, the zone of inhibition was found to increase with increase in concentration of $ZnFe_2O_4$ NPs. One possible mechanism of the antifungal action by the $ZnFe_2O_4$ NPs may be due the action of ROS and the induction of oxidative stress on fungal strain. This oxidative stress may disable ant proteases while at the same time activating metalloproteases, thereby encouraging proteolysis and uncontrolled cell destruction. Inflammation may accelerate the production of ROS and reduce the antioxidant defensive capacity, promoting oxidative stress and the associated tissue damage.

Conclusions

The experiment reporting the use of natural source and easily available capping agents clearly provides environmental friendly reproducible bio product. The synthesis of zinc ferrite nanoparticles was carried out successfully by eco-friendly biological reduction route. Detailed characterisation techniques imply the purity of the sample and phase formation was achieved by this green method. Especially morphological study reporting the applicable morphology of the sample is due to its ultrafine, spherical and close particle assembly. Metal-metal bonding and metal-oxygen bonding nature was viewed by FT-IR tool. Green derived zinc ferrite sample was undertaken for investigation of its antimicrobial behaviour. The zones of inhibition were formed in the antimicrobial screening test indicated that the sample shows good antibacterial and antifungal activity against various bacteria and fungi. Bio derived zinc ferrite

sample could be of immense use in medical field for their efficient antimicrobial function.

Acknowledgement

The Authors convey their heartfelt thanks to DST-FIST (SR/FST/CSI-003/2016) for the grant provided to procure the required instruments and infrastructure at the Chemistry Department of Vijayanagar Sri Krishnadevaraya University Ballari. Our thanks are also due to Prof. A. Venkataraman, Department of Chemistry, Gulbarga University, Kalaburagi for his support

References

1 Ali A, Zafar H, Zia M, Haq U I, Phull A R, Ali J S & Hussain A, *Sci Tech*, 9 (2016) 49.
2 Hussain I, Singh N B, Singh A, Singh H & Singh S C, *Biotech Lett*, 38 (2016) 545.
3 Jagadeesan A K, Duvuru J A, Anuradha J S, Ponnusamy S K, Kabali V A, Gopakumaran N, Selvaraj K R N, Thangavelu K, Sunny S, Somasundaram P P & Devarajan Y, *J Cleaner Pro*, 324 (2021) 129.
4 Fernández-García M & Rodríguez J A, *Encyclopedia of Inorganic and Bioinorganic Chemistry*, (Wiley Interscience, A John Wiley & Sons, INC) 2007, p. 15.
5 Sabir S, Muhammad A & Chaudhary S K, *Sci World J*, 1 (2014) 194.
6 Gupta D, Boora A, Thakur A, Gupta T K, *Rec Adv Lim*, *Env Res*, 231 (2023) 116316.
7 Thunugunta T, Reddy A C & Reddy L D C, *Nano Tech Rev*, 4 (2015) 303.
8 Kmita A, Pribulova A, Holtzer M, Futas P & Roczniale A, *Arch Met Mat*, 61 (2016) 2141.
9 Noguera C, *Physics and Chemistry at Oxide Surfaces*, (Cambridge University Press: Cambridge, UK), 1996, p. 128.
10 Rodriguez J A, Dvorak J, Jirsak T, Liu G, Hrbek J, Aray Y & González C, *J Am Chem Soc*, 127 (2002) 47.
11 Gafton E V, Bulai G, Caltun O F, Cervera S, Macé S, Trassinelli M, Steydli S, Vernhet D, *App Surface Sci*, 379 (2016) 171.
12 Naseri M G, Saion E B, Hashim M, Shaari A H & Ahangar H A, *Solid State Comm*, 151 (2011) 1031.
13 Husain S, Amin A M M, Soliman Y M M, S.I. El-Dek, Ahmed Y M Z & Zaki A H, *J Magnet Mag Mat*, 544 (2022) 168681. (https://doi.org/10.1016/j.jmmm.2021.168681).
14 Rachna N B & Agarwal A S, *Mat Today: Pro*, 5 (2018) 9148.
15 Kim W & Saito F, *Powder Tech*, 114 (2001) 12.
16 Nguyen L T T, Nguyen K D M, Nguyen T A & Kwangsoo N, *Ceramics Int*, 48 (2022) 4090.
17 Latif S, Amna L, Muhammad I, Javaid A, Hussain N, Jesionowski T & Muhammad B, *Env Res*, 216 (2023) 114500.
18 Karcioglu K Z, *Env Res Tech*, 4 (2021) 42.
19 Sahoo P, Choudhary P, Suvra S L, Dixit A & Mefford T, *Chem Comm*, 59 (2023) 12065.
20 Raghvendra S Y, Ivo K, Jarmila V, Jaromir H, Lukas K, Pavel U, Michal M, David S, Milan M & Martin H, *Ultrasonics Sonochemistry*, 40A (2018) 773. (https://doi.org/10.1016/j.ultsonch.2017.08.024).
21 Somvanshi S B, Kharat P B, Khedkar M V & Jadhav K M, *Ceramics Int*, 46 (2020) 7642.
22 Maiti D, Saha A & Devi P S, *Phy Chem Chem Phy*, 18 (2016) 1439.
23 Sriramulu M, Shukla D & Sumathi S, *Mat Res Exp*, 5 (2018) 115404.
24 Hao T, Maaza M & Ezema F I, *J Nano Res*, 23 (2021) 47.
25 Liaskovska M & Tatarchuk T, *Mol Cry Liq Cry*, 719 (2021) 45.
26 Basavanagoudra H, Tanakanti R, Patil M K, Inamdar S R & Goudar K M, *Macromol Symp*, 400 (2021) 2100138.
27 Basavaraja S, Balaji S D, Lagashetty A, Rajasab S & Venkataraman A., *Materials Research Bulletin*, 41 (2008) 1162.
28 Din M I, Jabbar S, Najeeb J, Khalid R, Ghaffar T, Arshad M, Khan S A & Ali S, *Int J Phytoremed*, 22 (2020) 1440.
29 Lakshmi R V, Pramila S, Nagaraju U G, Surendra B S & Mallikarjunaswamy C, *J Mat Sci: Mat Ele*, 31 (2020) 17386.
30 Lagashetty A K, Ganiger S K, Preeti R K, Reddy S & Malathesh P, *New J Chem*,14 (2020) 14095.
31 Lagashetty A K, Sangappa K & Reddy G S, *Heliyon*, 5 (2019) e02794.
32 Liaskovska M & Tatarchuk T, *Mol Cry Liq Cry*, 719 (2021) 45.
33 Nguyen N T T, Nguyen T T T, Nguyen D T C & Tran T V, *Sci Total Env*, 872 (2023) 162212.
34 Bayahia H, *J King Saud Uni – Sci*, 35 (2023) 102584.
35 Lagashetty A K, *Resonance*, 27 (2022) 1923.
36 Lagashetty A K, Ganiger S K, Preeti R K, Reddy S, *Bioint Res App Chem*, 11 (2020) 8087.
37 Tanuja G, Ganiger S K, Shashidhar, Preeti R K, Patil S R & Lagashetty A K, *Curr Chem Lett*, 12 (2023) 821.
38 Banerjee S, Chakravorty D, *AIP Conf Pro*, 1447 (2012) 233.
39 Okoroh D, Ozuomba J, Aisida S & Asogwa P, *Adv Nanopart*, 8 (2019) 36.
40 Swamy P, Basavaraj S, Lagashetty A K, Rao N V S, Nijgunappa R & Venkataraman A, *Bull Mat Sci*, 34 (2009)1325.
41 Lee P C, Chu C C, Tsai Y-J, Chuang Y-C & Lung F-D, *Chem Bio Drug Des*, 94 (2019) 1537.
42 Gabrielyan L, Hakobyan L, Hovhannisyan A & Trchounian A, *J App Microbio*, 126 (2019) 1108.
43 Aguilera L D S, Marcal R L S B, Campos J B, Silva M H P & Figueiredo A B S, *J Mat Res Tech*, 7 (2018) 350.
44 Murthy & A Merga, *Rev Adv Mat Sci*, 59 (2020) 464.
45 Wahab R, Kim Y-S, Mishra A, Yun S II & Shin H-S, *J Nano Res Lett*, 5 (2010) 1675.